Journal of Dynamics, Monitoring and Diagnostics, 2024, 3, 32-39
https://doi.org/10.37965/jdmd.2024.512

ISTP
RESEARCH ARTICLE

A Two-step Inverse Method for Quantitative Damage Evaluation of Plate-like Structures Using Vibration Approach

Shuai He,[1] Jiaxin Li,[1] Xuejing Wu,[1] Chunhui Wang,[2] and Tianran Lin[1]

[1]Qingdao Key Rail Transportation Laboratory for Noise and Vibration Control & Automated Fault Diagnostic, Qingdao University of Technology, Qingdao 266520, China

[2]School of Mechanical and Manufacturing Engineering, The University of New South Wales, Kingston 2052, Australia

(Received 23 January 2024; Revised 26 February 2024; Accepted 20 March 2024; Published online 20 March 2024)

Abstract: This study presents a novel two-step approach to assess plate-like structural laminar damages, particularly for delamination damage detection of composite structures. Firstly, a 2-D continuous wavelet transform is employed to identify the damage location and sizes from vibration curvature data. An inverse method is subsequently then used to determine the bending stiffness reduction ratio along a specified direction, enabling the quantification of the delamination severity. The method employed in this study is an extension of the one-dimensional inverse method developed in a previous work of the authors. The applicability of the two-step inverse approach is demonstrated in a simulation analysis and by an experimental study on a cantilever composite plate containing a single delamination. The inverse method is shown to have the capacity to reveal the detailed damage information of delamination within a constrained searching space and can be used to determine the effective flexural stiffness of composite plate structures, even in cases of complex delamination damage.

Keywords: 2-D continuous wavelet transform; damage quantification; delamination damage; inverse method; vibration

I. INTRODUCTION

Delamination, a prevalent problem in fiber composites, can significantly affect the material properties such as stiffness and strength of a composite structure [1]. The problem has attracted substantial interest from both academic and industry to develop reliable techniques for the detection and quantification of the delamination to evaluate the remaining strength and the remaining lifespan of a composite structure. Vibration-based techniques, renowned for their non-invasive characteristics, are extensively used in many industries for damage detection and quantification such as damage detection and assessment of delamination. Prior studies conducted by Zou *et al.* [2] and Fan and Qiao [3] investigated the use of vibration-based methods for delamination damage detection. Several other algorithms have also been suggested in the last twenty years, the majority of them offer only limited qualitative information on the kind and extent of delamination damage. For instance, Lestari *et al.* [4] presented a beam model that characterizes a damage as a beam section with decreased bending stiffness. They then solved the model analytically using a perturbation technique. However, it is important to note that the model is only applicable to small-scale damage. On the other hand, Maranon *et al.* [5] presented a six-step methodology for determining the location, dimensions, and depth of a solitary delamination inside a composite panel. However, it is uncertain whether the proposed procedure can be applied for impact damage detection involving several delamination within the thickness of the laminate.

Several other techniques based on the laminar theory have also been proposed to estimate the elastic characteristics of a composite structure with a particular arrangement between layers. One example is the initial estimation approach using the efficiency factor to quantify the overall contribution of each lay-up layer of a laminate at the angle θ. In addition, a method using a two-dimensional (2D) continuous wavelet transform to identify and separate delamination damage was presented in Refs. [6,7]. Furthermore, Fan and Qiao [8] presented a method for detecting delamination damage in a plate-like structure using the "Dergauss2d" wavelet in a continuous wavelet transform. It was shown that their method can have a better performance under the conditions of noise interference and limited sensor data compared with the 2-D gapped smoothing method [9] and the 2-D strain energy method. To extract the damage-induced local shape characteristics of plates, Yang *et al.* [10] introduced a low-rank and sparse data format for the 2-D strain field, which allows for the extraction of local shape properties in plates that have been damaged. However, it is noted that the finite difference approach used in the above analysis has the potential impact to decrease the estimation accuracy on the spatial derivatives of typical defection shapes (CDS). Several strategies have been proposed to tackle this problem [11–15]. Nevertheless, these strategies cannot warrant the accurate localization of the damage. In a recent study, Cao *et al.* [16] used a low-rank structure of a 2-D CDS and the sparse placement of the damage-induced characteristic to evaluate the baseline-free damage localization index which minimizes the impact of measurement noise and the truncation error of finite difference calculation. However, their approach is not able to disclose the extent of the damage.

Corresponding author: Tianran Lin (e-mail: trlin@qut.edu.cn).

Cao *et al.* [17] introduced a multi-objective algorithm that outperforms the traditional MOSA algorithms in terms of efficiency. Zhou *et al.* [18] presented a multi-level scheme modeling approach by applying a multi-objective optimization in the inverse model updating analysis and proved the algorithm is effective in detecting small-sized damage in composite materials. Meanwhile, Zhang *et al.* [19] presented a multi-objective optimization framework that utilizes piezoelectric impedance to pinpoint both the location and the severity of a damage. The multi-objective inverse approaches discussed above have successfully narrowed down the analysis to a small set of solutions that can accurately encompass the actual damage scenario. However, it is also noted that the works mentioned above, which employ the inverse method, could incur significant computational costs. Another limitation of the works is the capacity to evaluate the severity of a damage. In this study, we develop a two-step inverse method aiming for a swift identification and severity evaluation of a delamination damage in composite materials. The boundary of the damage obtained from Step 1 of the approach can serve as the input in Step 2, which will reduce the computational cost considerably than that of the previous studies.

The remainder of the paper is organized as follows: Section II reviews the theoretical base for plate-like structural laminate damage detection and quantification. Section III elaborates the detailed procedure of the proposed method and the solution framework. The proposed technique is validated in the analysis of a computer-simulated data in Section IV and by the analysis of an experimental test data in Section V. Section VI summarizes the main findings from this work.

II. THEORETICAL PRINCIPLES

It has been shown in a prior study [1] that the deflection curvature data is sensitive to tiny delamination damage which can be used to disclose the border of delamination damage in one-dimensional (beam-like) structure. For a one-dimensional structure such as beams, the curvature w'', the second-moment derivative of the displacement w, can be computed as $\partial^2 w/\partial x^2$. However, in the case of two-dimensional plate-like structures, the second-moment derivatives of the displacement profile are directional, consisting of $\partial^2 w/\partial x^2$, $\partial^2 w/\partial x \partial y$ and $\partial^2 w/\partial y^2$. Therefore, in order to fully understand the extent of the damaged area, it is crucial to take into account the directionality of each curvature component. Figure 1 is an example showcasing the three curvature components of the displacement profile of a rectangular plate. The dimensions of the rectangular plate used in this example are 140 mm by 280 mm where a square delamination damage of the size 14 mm by 14 mm is assumed.

III. A TWO-STEP INVERSE METHOD

The technique presented in this study for delamination damage detection of a two-dimensional laminar plate is

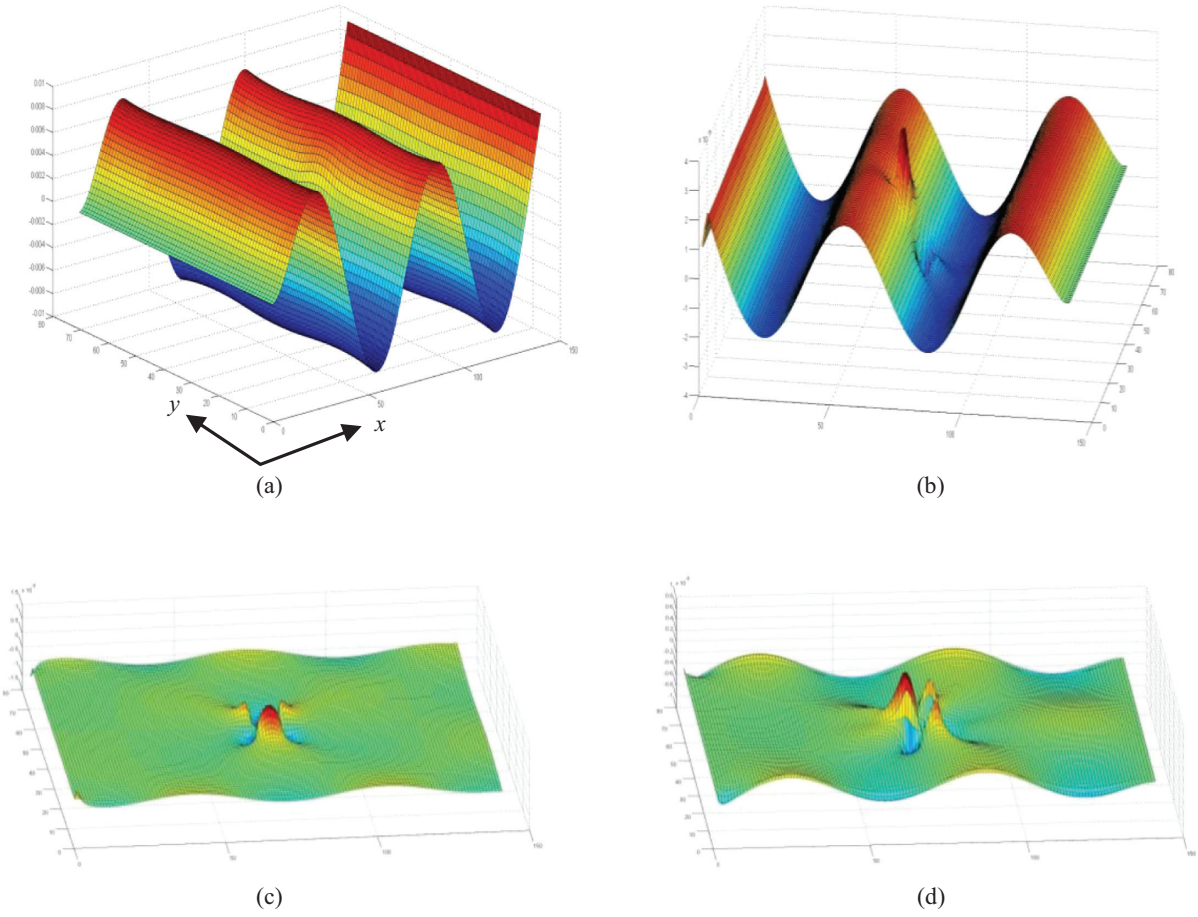

Fig. 1. The displacement profile of a rectangular plate containing a 14 mm × 14 mm delamination damage and the corresponding curvature data: (a) the displacement profile, (b) w''_{xx}, (c) w''_{xy}, and (d) w''_{yy}.

an extension of the two-step inverse approach developed in a prior work of the authors [1]. The main objective in the first step of the approach is to establish the precise extent of a delamination damage in a plate-like composite structure, which is then served as the input for the second step of the approach in which the objective is to determine the number and the through-thickness location of the delamination. The detailed approach of the two-step inverse method is elaborated as follows.

A. DAMAGE DETECTION USING A 2D CONTINUOUS WAVELET TRANSFORM – STEP 1

The damage detection technique of a plate-like composite structure based on the continuous wavelet transform is introduced in this section. The 2-D wavelet is defined in the following manner:

$$\psi_{u,v,s}(x,y) = \frac{1}{s}\psi\left(\frac{x-u}{s}, \frac{y-v}{s}\right) \tag{1}$$

where u and v are the translational parameters in the x and y-directions respectively, s is the scale parameter and $\psi(x,y)$ is the mother wavelet; here, the "Dergrauss2d" wavelet is selected according to the recommendation of Fan and Qiao [8]. In addition, a rotational parameter is provided for a plate-like structure.

$$\psi_{u,v,s}\left(x',y'\right) = \frac{1}{s}\psi\left(\frac{x'-u}{s}, \frac{y'-v}{s}\right) \tag{2}$$

here

$$\begin{bmatrix} x' \\ y' \end{bmatrix} = \begin{pmatrix} \cos\theta & \sin\theta \\ -\sin\theta & \cos\theta \end{pmatrix} \begin{bmatrix} x \\ y \end{bmatrix} \tag{3}$$

The 2D wavelet transform of a function $f(x)$ can be expressed as:

$$W_{wavelet} f(u,v,s,\theta) = \frac{1}{s}\int_{-\infty}^{+\infty}\int_{-\infty}^{+\infty} f(x,y)\psi\left(\frac{x-u}{s}, \frac{y-v}{s}\right)\mathrm{d}x\mathrm{d}y \tag{4}$$

The "Dergrauss2d" wavelet is essentially the derivative of the original Gaussian wavelet of the following form:

$$g^0(x,y) = \left(\sqrt{\pi/2}\right)^{-1} e^{-\left(x^2+y^2\right)} \tag{5}$$

It was found in Ref. [1] that the direct measured deflection data of a beam-like structure is not sensitive enough to detect a minor damage due to the interference of the background noise in the measurement. As a result, the curvature data, the second-moment derivative of the displacement data, which is sensitive to the change of flexural stiffness caused by damage, are adopted for the damage detection of the structure. Thus, in the first step of the approach, instead of calculating the derivatives of the measured displacement directly, the derivative of the wavelet function is computed. The derivative of the Gaussian wavelet function given by Equation (5) can be expressed as:

$$g^{m,n}(x,y) = \frac{\partial^{m+n}}{\partial x^m \partial y^n} g^0(x,y) \tag{6}$$

The following 2-D wavelet functions can be obtained for $g^{m,n}(x,y)$:

$$g^{m,n}_{u,v,s}(x,y) = \frac{1}{s} g^{m,n}\left(\frac{x-u}{s}, \frac{y-v}{s}\right) \tag{7}$$

To locate the damage in plate-like composite structures, the choice of the parameters $m = n = 2$ will render the best performance according to a systematic analysis presented by Qiao and Cao [8].

B. DAMAGE EXTENT ASSESSMENT – STEP 2

In order to lessen the computational burden, the inverse approach suggested by He *et al.* [1] for a beam-like structure is extended to two-dimensional plate-like structures in this study.

A schematic illustration of a cantilever rectangular plate is shown in Fig. 2. The governing partial differential equation for the bending displacement of the plate due to a line distributing force excitation applied along the free edge is:

$$D_x \frac{\partial^4 w}{\partial x^4} + 2H\frac{\partial^4 w}{\partial x^2 \partial y^2} + D_y \frac{\partial^4 w}{\partial y^4} = q\delta(x - L_x) \tag{8}$$

where w is the out-of-plane displacement of the plate, D_x and D_y are the bending stiffnesses along the x and y directions respectively, and $H = \upsilon_2 D_x + 2D_{xy} = \upsilon_1 D_y + 2D_{xy}$ denotes the effective torsional rigidity. δ signifies a Dirac delta function and L_x is the length of the plate in the x-direction.

The internal moments and shear forces of the plate resulting from the external force excitation can be expressed as:

$$M_x = -\left(D_x \frac{\partial^2 W}{\partial x^2} + \upsilon_2 D_x D_x \frac{\partial^2 W}{\partial y^2}\right) \tag{9}$$

$$M_y = -\left(D_y \frac{\partial^2 w}{\partial y^2} + \upsilon_1 D_y \frac{\partial^2 w}{\partial x^2}\right), \tag{10}$$

$$M_{xy} = -2D_{xy}\frac{\partial^2 w}{\partial x \partial y} \tag{11}$$

$$Q_x = -\frac{\partial}{\partial x}\left(D_x \frac{\partial^2 w}{\partial x^2} + H\frac{\partial^2 w}{\partial y^2}\right), \tag{12}$$

and

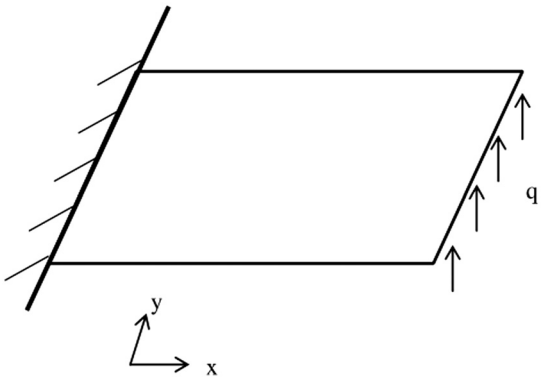

Fig. 2. A schematic illustration of a cantilever plate.

$$Q_y = -\frac{\partial}{\partial y}\left(D_y \frac{\partial^2 w}{\partial y^2} + H\frac{\partial^2 w}{\partial x^2}\right) \tag{13}$$

Here, M_x, M_y, Q_x, and Q_y represent the bending moments and shear forces, respectively.

To avoid the effect of the coupled bending stiffness in the two plate directions, a symmetrical loading condition is used as the external excitation, as seen in Fig. 3. Under this specific loading condition, the curvature value in the x-direction $\partial^2 w/\partial x^2$ plays a more significant role than the curvature value in the y direction $\partial^2 w/\partial y^2$. Equation 12 may thereafter be simplified as

$$Q_x = -D_x \frac{\partial^3 w}{\partial x^3} \tag{14}$$

Hence, the information from the undamaged structure can then be used as the baseline to compute the stiffness reduction ratio at the x-direction:

$$\frac{D_{x(d)}}{D_{x(0)}} = \frac{Q_{x(d)}}{Q_{x(0)}} \frac{w'''_{xxx(0)}}{w'''_{xxx(d)}} \tag{15}$$

where the subscript 0 refers to the undamaged structure, while the subscript d represents the structure containing delamination damage, and w'''_{xxx} specifies the third derivative of the deflection data in the x direction.

The slope ratio of the curvature data can be derived from the experimental measurement, whereas the shear force ratio can be determined by using the equilibrium equation as follows:

$$\frac{Q_{(0)}}{Q_{(d)}} = \frac{q + \int M\omega^2 w_0 dx}{q + \int M\omega^2 w_d dx} \tag{16}$$

where M represents the discrete element mass of the model. It is noted that the line distributing load q in Equation (16) will be replaced by a point force $F(t)$ in the experiment to signify the excitation through the vibration shaker applied at the mid-span of the plate at $y = \frac{L_y}{2}$ where L_y signifies the width of the plate.

It is important to note that Equation (16) applies solely to statically determinate structures, where it is possible to determine the internal shear force using different measured variables. In these conditions, the shear force in the y direction is considered to be minimal. The motion equation can be articulated through the Euler-Bernoulli beam theory, in which $M\omega^2 w(x)$ is equivalent to $EIw''''(x)$. Consequently, Equation (16) is useful for calculating the stiffness reduction ratio in a specific direction of a plate. This, in turn, facilitates the precise identification of delamination locations across the plate's thickness.

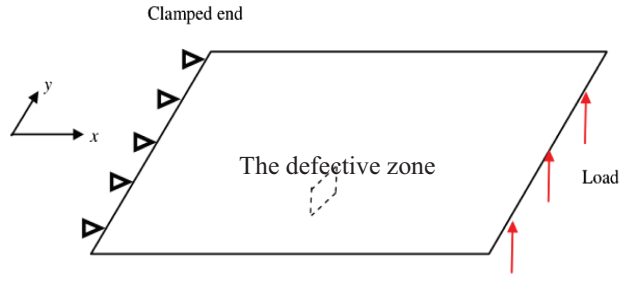

Fig. 3. A schematic illustration of the boundary and load condition of the plate.

IV. NUMERICAL ANALYSIS

This section illustrates how the suggested two-step inverse method is applied to identify damage in a two-dimensional, plate-like composite structure, leveraging simulated data obtained through finite element analysis (FEA). Here, a mid-plane delamination was simulated within the composite structure and calculated the resultant decrease in stiffness. The deflection data from this numerical model are assumed to be without noise, providing a baseline for comparison with experimental data discussed in the following section.

A delaminated plate model is generated using the commercial finite element software, Abaqus. The overall plate dimensions (Length × Width × Thickness) are assumed to be 280 mm × 140 mm × 3.36 mm, as shown in Fig. 4(a). The plate model consists of 16 fiber layers arranged in a stacking sequence of $[0,90]_{4s}$. Quadratic 3-D solid elements with an element surface size of 2 mm × 2 mm are used to mesh the plate model, and the depth of the element is the same as each fiber layer in the FEA modeling. For simplicity of the analysis, only a single delamination is considered in the study. The delamination has a square form and is positioned at a 45-degree angle to the x-axis which is created by changing the element connectivity as shown in Fig. 4(b). In addition, the 'hard-contact' boundary constraint is used in the simulation to prevent the penetration of elements in the FEA model. Clamped boundary condition is applied to the plate edge at $x = 0$, while the other plate edges are kept unconstrained, as shown in Fig. 3. Single frequency (8.4 kHz) sinusoidal line distributing normal excitation force is applied along the free edge of the plate at $x = L_x$ in the simulation.

As mentioned in the theoretical section, the 2-D wavelet transform can be performed at different scales (s) and orientations (θ). Nevertheless, the values of θ and s are fixed to 0 and 5 correspondingly in the analysis for the illustration purpose. The plate deflection under this setting is shown in Fig. 5. The results demonstrate that the proposed method effectively identifies the damage location by analyzing the peak value in the coefficient plot (Step 1), while the second step in the approach involves the assessment of the damage's extent. The approach further allows for the determination of the delamination damage's size and shape, details of which are elaborated in the subsequent section.

To quantify the severity (size) of the delamination damage, it is necessary to calculate the ratio of slopes and the ratio of shear forces as specified in Equation (15) to determine the decrease in plate flexural stiffness in the x-direction. The curvature profile in the x-direction (w''_{xx}) can be calculated by differentiating the plate displacement function twice with respect to x. The calculated curvature profile as shown in Fig. 6 clearly reveals the presence of abnormalities, and the delamination damage is situated between $y = 40$ mm to $y = 60$ mm along the y direction. Figure 7 shows a comparison result by comparing the curvature profile of the delaminated plate at $y = 48$ mm together with the displacement profile of the undamaged structure at the same location. These two curvature profiles (blue line and red line) intersect at $x = 140$ mm. The slope ratio at the intersection point can be obtained by taking the derivative of these two displacement curves at the intersection, resulting in $\frac{w'''_u}{w'''_d} = 0.2152$.

On the other hand, the shear force ratio can be calculated using Equation (16). In this particular scenario,

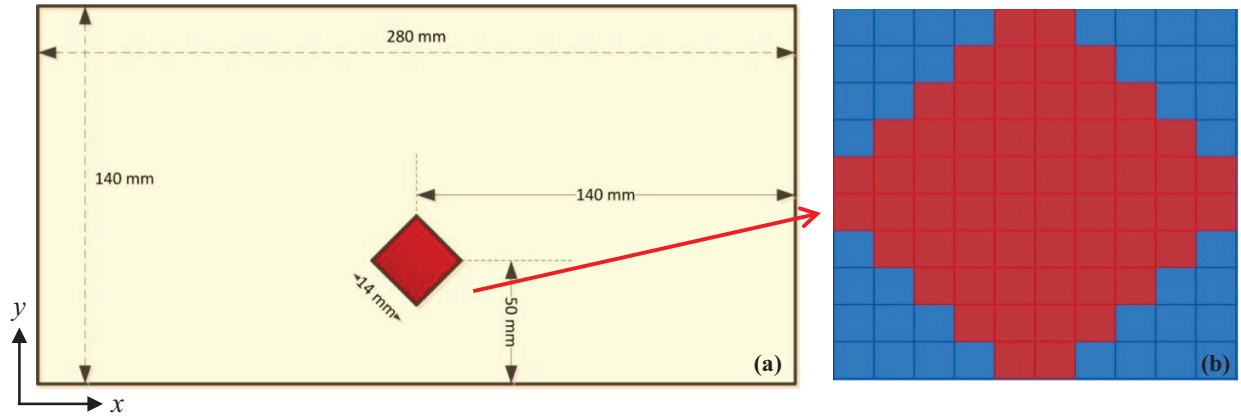

Fig. 4. A schematic illustration of a composite plate containing a square delamination, (a) the top view of the rectangular plate, and (b) the enlarged view of the damage region.

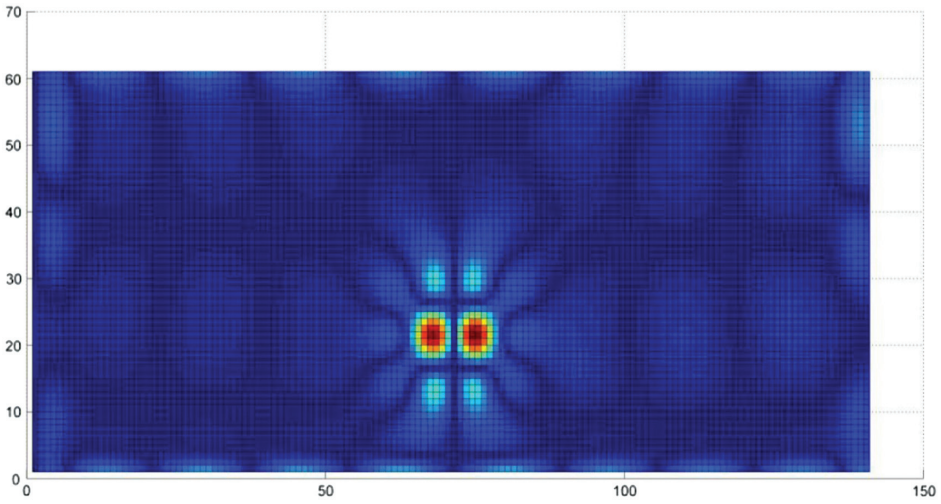

Fig. 5. The 2-D continuous wavelet coefficients of the deflection profile ($s = 5$).

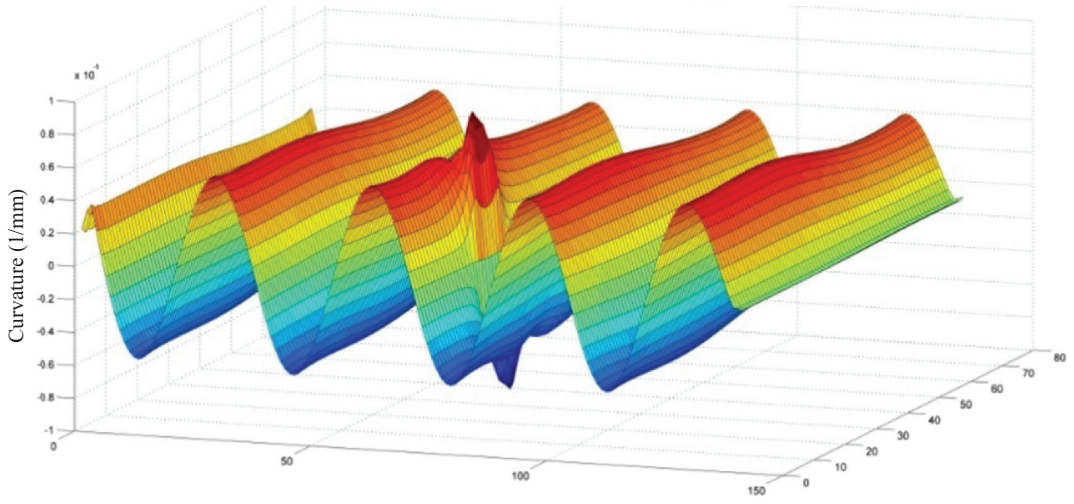

Fig. 6. The curvature profile w''_{xx} for the damaged structure at 8.4 kHz.

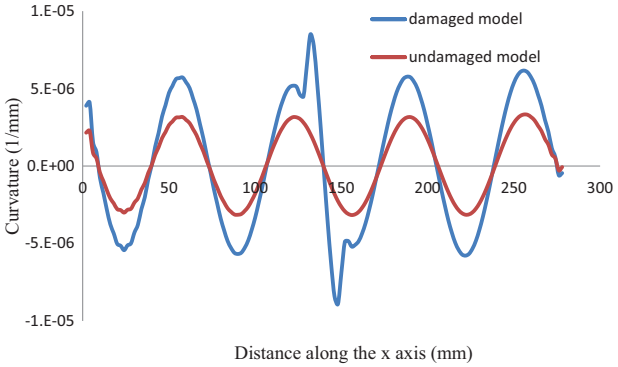

Fig. 7. A comparison of the curvature profiles of the damaged and the undamaged plate at $y = 48$ mm.

the ratio of the downward shear stress ($\boldsymbol{Q_x(d)}$) to the upward shear stress ($\boldsymbol{Q_x(u)}$) is 1.122, resulting in a stiffness reduction ratio in the x-direction, $\frac{\boldsymbol{D_x(d)}}{\boldsymbol{D_x(u)}} = 0.243$.

V. EXPERIMENTAL VALIDATION

This section details an experimental investigation using a composite plate specimen, which features a circular mid-plane delamination as depicted in Fig. 8. The stacking sequence of this plate specimen mirrors that of the numerical model used in the study. The impact of the delamination on stiffness reduction is significantly influenced by its through-thickness location. Therefore, the experimental findings can be directly compared to the outcomes of the numerical model.

The dimensions of the plate specimen are 140 mm × 280 mm × 3.36 mm which has a layer stacking sequence of $[0, 90]_{4s}$. An undamaged plate specimen with same material properties and dimensions was also manufactured to be used as the reference.

Artificial delamination damage was created by embedding two layers of thin Teflon films into the mid-plane in one of the composite plate during the manufacturing process. Prior to curing, the specimens were enclosed in a vacuum bag and then subjected to a curing process inside an autoclave at a temperature of 120 °C and a pressure of 90 psi for a duration of 1 hour. The specimens were manufactured with unidirectional carbon-fiber epoxy prepreg T700/VTM 264 whose material properties are listed in Table I.

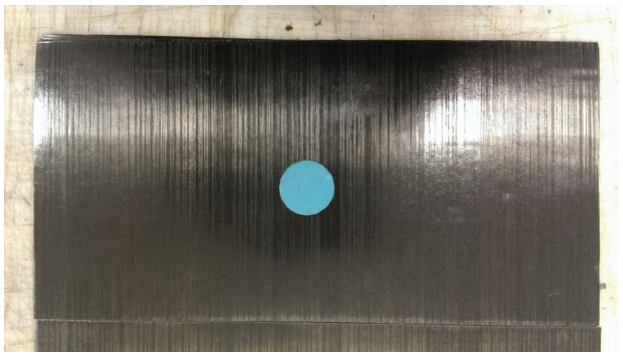

Fig. 8. An illustration of the Teflon disc on a ply surface.

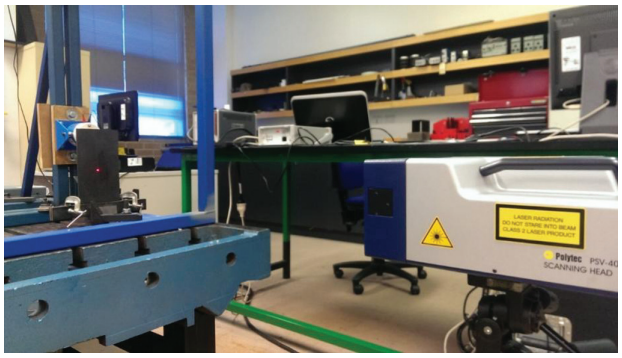

Fig. 9. The experimental test setup.

During the curing process, the resin might flow into the interface between the Teflon films due to the high autoclave pressure. The resin can cause the two Teflon films to stick to each other and to the composite after the curing process. In order to ensure full separation between the Teflon films and the composite laminate, plate specimens were pre-loaded under controlled compression-shear loading before testing.

The experimental setup is shown in Fig. 9. The specimen was clamped in a fixture at one end and driven at the other end by a mechanical shaker. Measurements of the out-of-plane velocity response were acquired by a scanning laser vibrometer – Polytec PSV400, from which the deflection-time data can be obtained. The measured deflection data are then used to compute the curvature data for damage localization and quantification purpose in this study. During the scanning process, a scanning grid consisting of 59 × 119 points was preconfigured in the computer, as seen in Fig. 10, this leads to a uniform spatial resolution of 2.2 mm in both plate directions. The AC input signal used to drive the mechanical shaker is also generated directly by the embedded Polytec operating software. A continuous sinusoidal signal at 8.4 kHz was applied to excite the composite plate.

The plate deflection profile measured by the laser scanner is then analyzed using the proposed two-step inverse technique. Prior to the analysis, a cubic interpolation method is used to enhance the resolution of the measured deflection profile from 2.2 mm to 1 mm. After that, the 2D continuous wavelet transform is employed on the enhanced experimental data, enabling the distinct identification of the embedded damage pattern amongst the background noise, as seen in Fig. 11. Irregularities can also be observed at locations close to the right edge of the plate which is caused by the near field effect closed to the location where the shaker head is attached.

The damage boundary was initially identified utilizing the previously mentioned CWT method. Subsequently, in Step 2, the severity of the delamination damage is assessed

Table I. Elastic properties of the T700/VTM264 unidirectional carbon/epoxy prepreg

E_{11}(GPa)	E_{22}(GPa)	E_{33}(GPa)	G_{12}(GPa)	G_{13}(GPa)	G_{23}(GPa)	ϑ_{12}	ϑ_{13}	ϑ_{23}
120.2	7.47	7.47	3.94	3.94	2.3	0.32	0.32	0.33

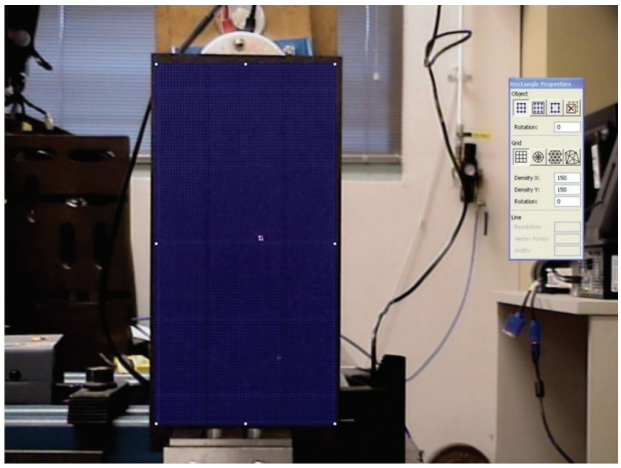

Fig. 10. The definition of the scanning grid points for the laser scanning.

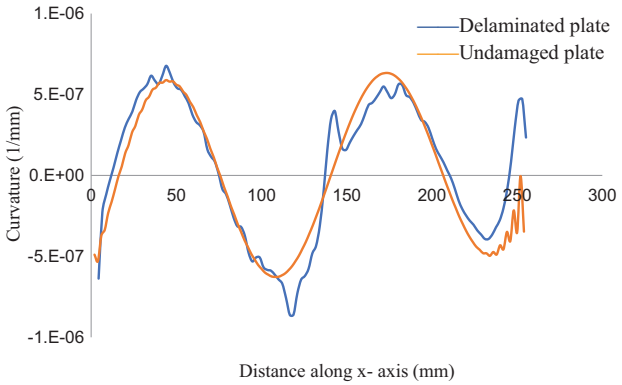

Fig. 12. The curvature profiles of the intact and the delaminated plates along the red dash line.

through the stiffness reduction method. Figure 12 presents a comparison of the curvature between damaged and undamaged plate specimens based on the measured profile and the pre-damage calculated curvature as reference points. This comparison follows the path marked by the red dashed line in Fig. 11. The area of the simulated circular damage having a 30 mm in diameter spans from 40 mm to 70 mm along the y-axis, while the position of the red dashed line is laying at 48 mm on the y-axis. The gradients of these two curvature profiles at the intersection point are determined to be $w_d''' = 8.21 \times 10^{-8}$ and $w_0''' = 2.97 \times 10^{-8}$ respectively which leads to a shear force ratio of $\frac{Q_{x(d)}}{Q_{x(0)}} = 0.9$ and a stiffness reduction ratio of 0.32. The through-thickness position of the delamination can then be estimated based on the stiffness reduction ratio, which is close to the mid-plane of the laminated plate.

The experimentally derived stiffness reduction ratio (0.32) is marginally greater than the numerical outcome (0.243), which aligns more closely with the theoretical prediction (0.25). This discrepancy may stem from the measurement noise associated with the spatial resolution of the laser vibrometer and the boundary condition of the setup in the experiment. Future research will be dedicated to a comprehensive analysis of these factors.

VI. CONCLUSIONS

A two-step inverse technique developed previously for delaminated damage detection of beam-like structures was successfully extended to the delaminated damage detection and quantification of plate-like composite structures. The efficacy of the technique is examined by using a numerical example and by the result of an experimental test. The results demonstrate that the border of delamination damage can be precisely determined by the analysis of the plate displacement profile data using the two-step inverse technique. The severity of the damage can be evaluated by comparing the slope of the displacement curvature in the damaged region of the plate with that of the undamaged plate. The result confirms that the proposed technique is capable of detecting both the delamination and its precise position.

CONFLICT OF INTEREST STATEMENT

The authors declare no conflicts of interest.

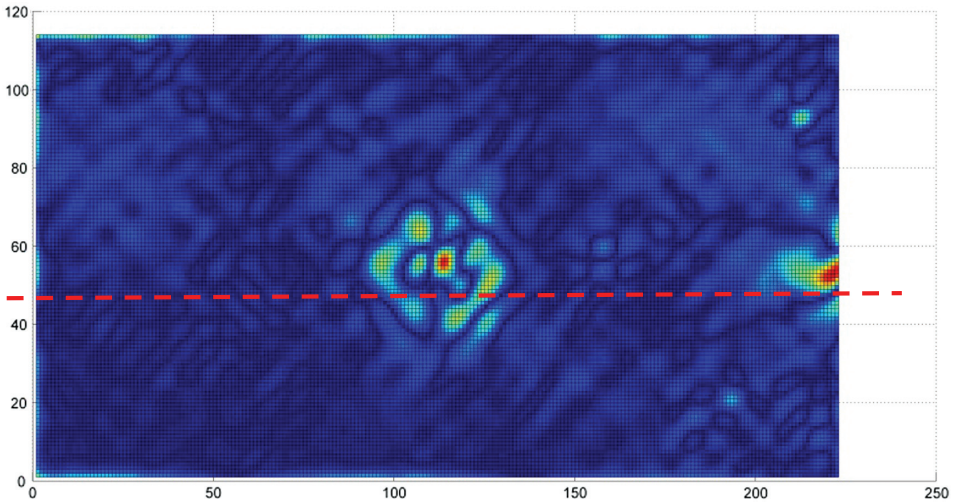

Fig. 11. The calculated wavelet coefficients of the measured deflection data.

REFERENCES

[1] S. He, L. R. F. Rose, and C. H. Wang, "Inverse methods for quantitative assessment of delamination damage based on vibrational response," *Struct. Health Monit.*, vol. 14, no. 5, pp. 411–425, 2015.

[2] Y. Zou, L. Tong, and G. P. Steven, "Vibration-based model-dependent damage (delamination) identification and healthy monitoring for composite structures – a review," *J. Sound Vib.*, vol. 230, no. 2, pp. 357–378, 2000.

[3] W. Fan and P. Qiao, "Vibration-based damage identification methods: a review and comparative study," *Struct. Health Monit.*, vol. 10, no. 1, pp. 83–111, 2011.

[4] W. Lestari, Q. Pizhong, and S. Hanagud, "Curvature mode shape-based damage assessment of carbon/epoxy composite beams," *J. Intell. Mater. Syst. Struct.*, vol. 18, no. 3, pp. 189–208, 2007.

[5] A. Maranon et al., "Identification of subsurface delaminations in composite laminates," *Compos. Sci. Technol.*, vol. 67, no. 13, pp. 2817–2826, 2007.

[6] E. Douka, S. Loutridis, and A. Trochidis, "Crack identification in plates using wavelet analysis," *J. Sound Vib.*, vol. 270, no. 1–2, pp. 279–295, 2004.

[7] M. Rucka and K. Wilde, "Application of continuous wavelet transform in vibration based damage detection method for beams and plates," *J. Sound Vib.*, vol. 297, no. 3–5, pp. 536–550, 2006.

[8] W. Fan and P. Qiao, "A 2-D continuous wavelet transform of mode shape data for damage detection of plate structures," *Int. J. Solids Struct.*, vol. 46, no. 25–26, pp. 4379–4395, 2009.

[9] M. K. Yoon et al., "Local damage detection using the two-dimensional gapped smoothing method," *J. Sound Vib.*, vol. 279, no. 1–2, pp. 119–139, 2003.

[10] Y. Yang, P. Sun, et al., "Full-field, high-spatial-resolution detection of local structural damage from low-resolution random strain field measurements", *J. Sound Vib.*, vol. 399, pp. 75–85, 2017.

[11] E. Sazonov and P. Klinkhachorn, "Optimal spatial sampling interval for damage detection by curvature or strain energy mode shapes," *J. Sound Vib.*, vol. 285, pp. 783–801, 2005.

[12] Z. Zhou, L. D. Wegner, and B. F. Sparling, "Vibration-based detection of small-scale damage on a bridge deck," *J. Struct. Eng.*, vol. 133, pp. 1257–1267, 2007.

[13] X. Jiang, Z. Ma, and W. Ren, "Crack detection from the slope of the mode shape using complex continuous wavelet transform," *Comput.-Aid. Civil Infrastruct. Eng.*, vol. 27, pp. 187–201, 2012.

[14] H. Lopes, R. M. Guedes, and M. Vaz, "An improved mixed numerical-experimental method for stress field calculation," *Opt. Laser Technol.*, vol. 39, pp. 1066–1073, 2007.

[15] H. Xu, L. Cheng, and Z. Su, "Suppressing influence of measurement noise on vibration-based damage detection involving higher-order derivatives," *Adv. Struct. Eng.*, vol. 16, pp. 233–244, 2013.

[16] S. Cao, H. Ouyang, and L. Cheng, "Baseline-free adaptive damage localization of plate-type structures by using robust PCA and Gaussian smoothing," *Mech. Syst. Signal Process.*, vol. 122, pp. 232–246, 2019.

[17] P. Cao et al., "A reinforcement learning hyper-heuristic in multi-objective optimization with application to structural damage identification," *Struct. Multidiscip. Opt.*, vol. 66, no. 1, p. 16, 2022.

[18] K. Zhou, Y. Zhang, and J. Tang, "Order-reduced modeling-based multi-level damage identification using piezoelectric impedance measurement," *IFAC-PapersOnLine,* vol. 55, no. 27, pp. 341–346, 2022.

[19] Y. Zhang, K. Zhou, and J. Tang, "Piezoelectric impedance-based high-accuracy damage identification using sparsity conscious multi-objective optimization inverse analysis," *Mech. Syst. Signal Process.*, vol. 209, p. 111093, 2024.